A new neutron single crystal diffractometer dedicated for biological macromolecules (BIX-4)

Kazuo Kurihara,[*] Ichiro Tanaka, Muhammad Refai Muslih,[†] Andreas Ostermann[‡] and Nobuo Niimura

Neutron Science Research Center, Japan Atomic Energy Research Institute (JAERI), Tokai, Ibaraki 319-1195, Japan. E-mail: kurihara@kotai3.tokai.jaeri.go.jp

We have constructed a new neutron single crystal diffractometer (BIX-4) at 1G-B port of JRR-3M in JAERI. Since at 1G-B port another diffractometer for biology, BIX-3 and a high-resolution powder diffractometer (HRPD) coexist, the monochromator house needed to be reconstructed. The main architecture of BIX-4 is based on that of BIX-3. BIX-4 uses an elastically-bent perfect-Si crystal monochromator and neutron imaging plates as BIX-3. In addition, several optimizations of the monochromator and modifications from previous BIX-3 are carried out. The final gain of the neutron intensity at the detector position is estimated to be 2.5 times larger than previous BIX-3. That higher performance increases the opportunities to apply neutron crystallography to biological macromolecules which give only weak reflections and/or small crystals.

Keywords: neutron crystallography; biological macromolecules; 3-plate assembled monochromator.

1. Introduction

Hydrogen atoms occupy about half of the atoms in a protein molecule, and water molecules of hydration always surround a protein. There is no doubt that they play an important role in physiological functions. They are indispensable substances in many biological processes. In addition, H atoms are intimately involved in the folding and stabilization of protein structure through hydrogen bonds. Therefore, the determination of accurate positions of hydrogen atoms of a protein and its hydration water molecules is an important information for understanding the mechanism, function, and stability of proteins (Niimura, 1999; Niimura *et al*., 2003).

In Japan Atomic Research Institute (JAERI) we have developed and installed new NIP-based diffractometers called BIX-2 in 1996 (Fujiwara *et al*., 1998) and BIX-3 in 1999 (Tanaka *et al*., 1999*b*) at T2-3 beam port in the thermal guide hall and at 1G-A beam port in the reactor hall of the JRR-3M, respectively. Especially using BIX-3 it has been possible to collect high-resolution diffraction data sets within about one month, and the diffractometer has been applied to the structure determination of rubredoxin from *Pyrococcus furiosus* in 1.5 Å resolution (6kDa) (Kurihara *et al*., 2001), its 3-point mutant in 1.6 Å (6kDa) (Chatake *et al*., 2002) and sperm whale myoglobin in 1.5 Å (16kDa) (Ostermann *et al*., 2002). Previous studies of the neutron protein crystallography and those recent results at JAERI have increased activity of this field (Tsyba & Bau, 2002). Therefore a much higher performance is now required to shorten the measurement time and/or get more accurate diffraction data.

Thus, we have constructed a new single-crystal diffractometer for neutron protein crystallography (BIX-4) at new 1G-B port of

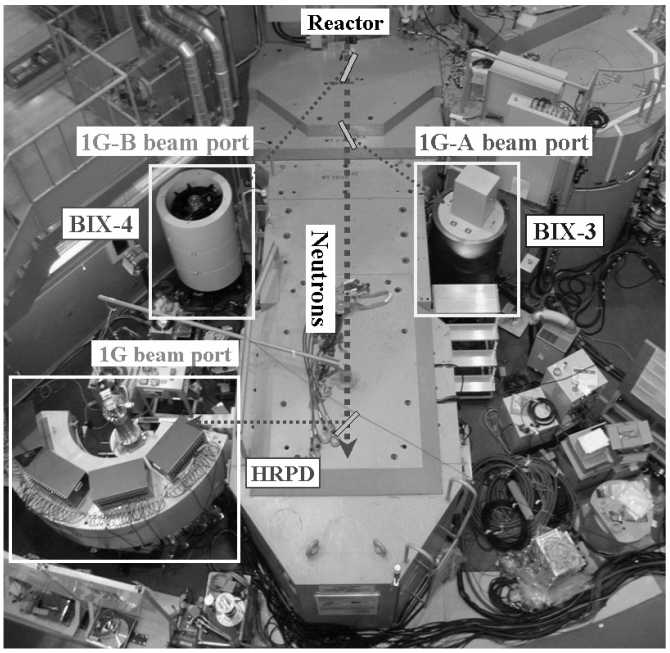

Figure 1

Top view around the neutron beam line shared with 1G, 1G-A and 1G-B beam in the reactor hall of JRR-3M. The dotted lines indicate the path of neutron beam from the reactor as a guide for the eyes. From up-stream BIX-4, BIX-3 and HRPD are arranged, and they used different wavelengths, 2.6 Å, 2.9 Å and 1.8 Å, respectively.

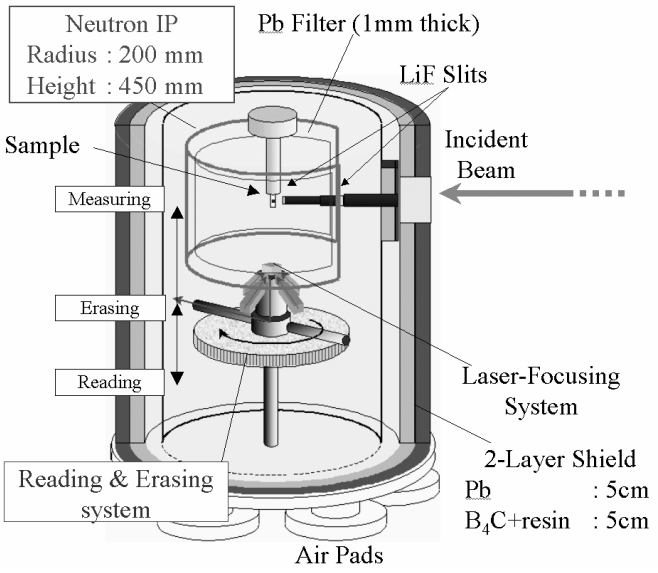

Figure 2

Schematic drawing of BIX-4. Neutron beam comes from right side. The neutron beam comes from the right side. During data collection the NIP is located at the top position. In the reading procedure the NIP cylinder moves down and is scanned by the laser with a reading rod rotating. After the reading the NIP moves up to the top position under exposure of an erasing lamp.

[†] Present address: P3IB-BATAN Gd.40 kawasan PUSPIPTEK Serpong Tangerang, Indonesia 15310.
[‡] Present address: Technische Universität München, ZWE FRM-II, Lichtenbergstrasse 1, D-85747 Garching, Germany.

Figure 3

The camera body of BIX-4 without cylinder shield (right), the NIP and laser modules (left top), and the reading rod and erasing lamp (left bottom). During the measurement the camera body is covered by the shield composed of two layers, one is a 50mm-thick B_4C + resin against neutrons, and the other is a 50mm-thick lead against γ-rays.

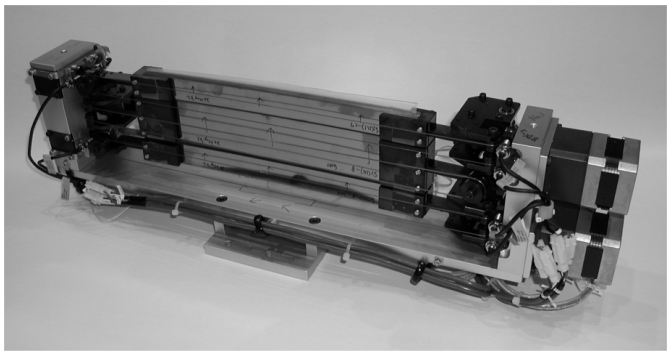

Figure 4

The new monochromator consists of three EBP-Si plates arranged in vertical. It covers the full size of neutron beam from the reactor. The tilt and $2\theta_M$ angles of the top and bottom plates can be changed individually.

JRR-3M of the JAERI. In order to get space for the monochromator and the flight tube of BIX-4 a portion of the monochromator house was reconstructed where 1G-A port is located and BIX-3 has been already installed. At this reconstruction the layout of 1G-A port was also changed because the monochromator position of BIX-4 was designed to be located close to that of BIX-3. Therefore, its monochromator position, $2\theta_M$-angle and so on were adapted accordingly although the BIX-3 camera body itself was not changed (hereinafter a name "previous BIX-3" is used for the BIX-3 before the reconstruction to distinguish from current BIX-3). As a result, the two diffractmeters are located at the opposite sides against the house each other as shown in Figure 1. The neutron beam line used for 1G-A/-B port is also shared with another beam port 1G for the high-resolution powder diffractometer (HRPD) located to the down-stream side from BIX-3/-4. However, since BIX-3 as well as the new installed BIX-4 use Si monochromators which have low absorption coefficient against thermal neutrons, and different wavelengths are used each other, all 3 instruments can coexist at this beam line.

The main architecture of BIX-4 is based on that of previous BIX-3. Figure 2 shows a schematic drawing of the camera body of BIX-4. The details of the architecture and the performance of previous BIX-3 is discussed elsewhere (Tanaka *et al*., 2002). BIX-4 also uses an elastically bent perfect Si (EBP) crystal monochromator (Niimura *et al*., 1995; Tanaka *et al*., 1999*a*) and a neutron imaging plate (NIP) (Niimura *et al*., 1994; Haga *et al*., 2002) as previous BIX-3. The NIP has a cylindrical shape and is arranged vertically, which makes the diffractometer compact and reduces the installation space. This is advantageous to solve following shielding problem: since the NIP is also sensitive to γ-rays, this instrument is shielded against γ-rays as well as neutrons. Thereby, BIX-4 works even in the reactor hall, where the γ-ray background is relatively high.

2. Design

2.1. Basic design

The basic design of BIX-4 instruments followed that of previous BIX-3. Figure 3 shows photos of the appearance of the camera body and the main parts of the instruments of BIX-4. The NIP covers a large solid angle subtended at the sample with a fine positional linearity, high spatial accuracy and good neutron detector efficiency. The circumference of NIP cylinder is 1,000 mm (range of $2\theta_S$ angle = ±140°), its height 450 mm, and the camera radius 200 mm. The read-out system itself consists of a laser-system which is 4-combined laser in total, and a photomultiplier system. The read-out procedure is performed in a rotating technique via a reading rod. To shield the neutron- and γ-background from the environment in the reactor hall the diffractometer is covered by a cylinder which consists of two layers, 50 mm-thick B_4C mixed with resin against neutron (outside) and 50 mm-thick lead against γ-rays (inside).

As a monochromator the EBP-Si crystal is used as previous BIX-3. This crystal is adopted to focus the reflected neutrons (radius of curvature is 4.1m) and serves to deliver more neutrons at the distant sample position. The monochromator is modified from that of previous BIX-3 before installing BIX-4 which is discussed at a next section.

2.2. Modification from previous BIX-3

At the reconstruction of the monochromator house and the installation of new BIX-4 several optimizations of the monochromator and modifications from previous BIX-3 are carried out as follows,

(1) The neutron beam from the reactor comes out through a collimator of 80 mm in height × 44 mm in width. However, only its bottom half was for the previous BIX-3 at the monochromator position. After the reconstruction of the monochromator house, a new monochromator composed of three EBS-Si plates is used to cover the full size of neutron beam (see figure 4). The dimension of the center plate is the same as for previous BIX-3 (250 mm in length × 40 mm in height × 10 mm in thickness). The top and bottom plates also have the same width and thickness, but 20 mm in height. They can be tilted independently to create a vertical focusing monochromator. In order to adjust the shifted direction of neutrons reflected on them by tilting, each of their $2\theta_M$-angles is also changeable by shifting in horizontal the position of one edge of the plate. These angle changes can be performed by remote control.

(2) A super mirror guide is installed inside of a flight tube to increase the intensity by reflecting thermal neutrons on the walls of the guide. The super mirror used for BIX-4 is composed of Ni/Ti

Table 1

Comparison of the specification of BIX-4 and previous BIX-3.

	BIX-4	Previous BIX-3
Monochromator	EBP-Si (111) / (311) Assembly of 3 plates	EBP-Si (111) / (311) Single plate
Wavelength	2.60Å / 1.36Å	2.35Å / 1.23Å
Used neutron beam size at monochromator	80 mm × 44 mm	40 mm × 44 mm
Monochromator to sample distance	225 cm	230 cm
Super mirror inside of flight tube	3.6Q	-
NIP size	450 mm × 1000 mm	450 mm × 1000 mm
Camera radius	200 mm	200 mm
d-min (along the horizontal)	1.38Å / 0.72Å	1.25Å / 0.65Å
Intensity at sample position (with Si(111))	4.5×10^6 n cm^{-2} s^{-1}	2.5×10^6 n cm^{-2} s^{-1}
$\Delta\lambda/\lambda$	0.021	0.015
Angular divergence	±1°	±0.5°
Estimated relative gain at detector position (with Si(111))	2.5	1
IP reading interval (in horizontal × in vertical)	0.1 mm × 0.1 mm / 0.2 mm	0.2 mm × 0.2 mm

multi-layers. Its critical angle of total reflection is proportional to the wavelength of neutrons and 6.1×10^{-3} rad/Å, so-called 3.6Q where Q is critical angle of Ni, 1.7×10^{-3} rad/Å.

(3) The angular divergence of the incident neutron beam is twice (about ±1°) as large as for previous BIX-3 because of the larger monochromator and the almost same distance between the monochromator and the sample (225 cm). This large divergence gets separation between Bragg reflections to be small. In order to reduce the limitation the wavelength for the incident neutrons 2.6 Å ($2\theta_M$ = 49°) is used instead of 2.35 Å ($2\theta_M$ = 44°) used by previous BIX-3 in the case of Si(111) monochromator for standard operation. According to this wavelength value the *d*-min value along the equator line, that is, the highest-possible resolution is 1.38 Å. At another option of Si(311) the wavelength and the *d*-min value are 1.36 Å and 0.72 Å, respectively.

(4) The *d*-min value at the top and bottom edges of the center of NIP is 3.17 Å. In order to get sufficient data completeness for higher-resolution data set than that value in vertical direction BIX-4 can set NIP at another position, 140 mm lower in height than at the standard measurement position, and then *d*-min value reaches to be 2.55 Å at the top and bottom edges of the center of NIP.

(5) In order to get better statistics of data measurement the read-and-output procedure of NIP is changed as follows. While in the horizontal direction the reading interval is shortened from 0.2 mm (previous BIX-3) to 0.1 mm, in the vertical direction one can select two modes, 0.1 mm or 0.2 mm. On the other hand, the spatial resolution in the stage of output is unchanged and 0.2 mm × 0.2 mm same as in previous BIX-3 by summing up the intensities of neighbor 4 or 2 points to a value for one pixel, respectively. However, the shortening of the interval along the vertical makes the time of NIP reading itself twice, which leads to 8 min in total for one cycle of reading/erasing procedure while 5 min in the case of 0.2-mm reading mode.

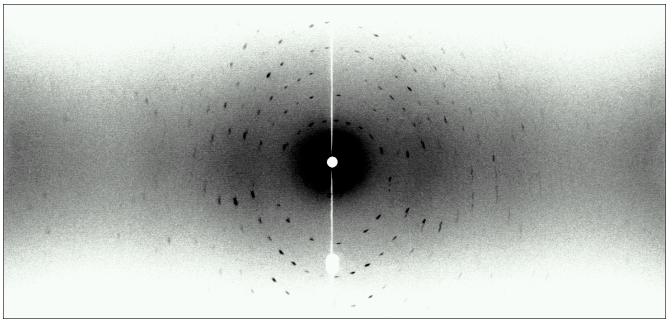

Figure 5

An example of the diffraction patterns taken by BIX-4. The sample is a sperm whale myoglobin crystal (volume = 6 mm^3). It was crystallized in H_2O and soaked in D_2O solution. Space group is $P2_1$ (a = 64.5Å, b =3 0.8Å c = 34.8Å, β = 105.7°). The exposure time was 1 hour. We can see diffraction spots up to 1.5 Å resolution.

3. Performance

3.1. Intensity and background

The comparison of specification between BIX-4 and previous BIX-3 is summarized at Table. 1. To compare the neutron intensities between them the intensities are measured by an off-line NIP. The intensity at the sample position of BIX-4 is derived to be 4.5×10^6 neutrons cm^{-2} s^{-1} which is 1.85 times larger than previous BIX-3. As the reflectivity of the sample is proportional to the 3rd power of the wavelength, the final gain for the integrated intensity of the Bragg spots are estimated to be 2.5 times larger. Supposing that 800 frames are measured for one data set with 60 min/frame, only 18 days is necessary for BIX-4 (at 0.1mm × 0.1mm reading) whereas 36 days are required in the case of previous BIX-3. On the other hand, the minimum crystal volume suitable for the measurement with BIX-4 leads to about 1 mm^3 instead of 2 mm^3 with previous BIX-3.

The contribution of top and bottom plates of the monochromator to the total intensity at the sample position is measured to be 57% which could include the effect of the super mirror. From these measurements the intensity on the detector position only from the center Si plate is estimated to be the almost same as for previous BIX-3.

On the other hand, the background of BIX-4 increases. Profiles of the background along the horizontal line around the direct beam height were measured with a tetragonal crystal of hen-egg-white lysozyme grown in D_2O solution as a typical sample. The comparison between BIX-4 and previous BIX-3 reveals that the background of BIX-4 is 2.5 times larger. Therefore, the ratio of the intensity over the background is almost the same as in the case of previous BIX-3. The same increase of the background as the intensity occurred because the most of the background is the unavoidable one from the sample. In BIX-4 and previous BIX-3 the background from outside of camera body was suppressed by the cylinder shield (§2.1) and additional shielding. Moreover, even if the ratio intensity to background of BIX-4 is the same as that of previous BIX-3, higher intensity in BIX-4 leads to a better data statistics than BIX-3 at the same measurement time.

3.2. Divergence and spot separation

The $\Delta\lambda/\lambda$ is estimated from FWHM of the monochromator rocking curve measurement. The result is 0.021 which is 1.4 times larger than 0.015, an estimated value for previous BIX-3 because the size of the new fright tube is larger than for the BIX-3 according to the new larger monochromator.

As mentioned in the previous section (§2.2), the large angular divergence of the incident neutron beam at BIX-4 introduces small distance between neighboring Bragg spots. As already discussed elsewhere (Tanaka *et al*., 1999*a*) the limit value of unit cell dimension of an imaginary cubic crystal is estimated to 55 Å whereas it be 90 Å for previous BIX-3. Therefore, in the case of the sample of large cell constants top and/or bottom plate of the monochromator would be set at off-angle to reduce the divergence of the incident beam. Even if the data is measured only with the center Si plate, BIX-4 gives the same performance as previous BIX-3 as mentioned in the previous section (§3.1). Here it should be noted that the above limit value is useful only as an index. In fact, cytochrome C' (14kDa) of 160 Å in *c*-axis has been measured using previous BIX-3 and the preliminary structure has been also solved (unpublished data).

3.3. Reading resolution

Incoherent scattering of H_2O was measured in the both cases of 0.1mm- and 0.2 mm-interval reading in NIP cylinder axis. The gain of the intensity and the signal-to-noise ratio is obtained to be 1.3 and 1.1, respectively. The 0.1 mm-interval reading needs additional 3 min for one read/erasure procedure. Therefore, this mode would be used for long exposure measurement, for example, 2 hours or more per frame.

4. Example of measurements

Figure 5 shows an example of the diffraction patterns from a myoglobin crystal. The white area at the center of that figure is the direct-beam position. We can see diffraction spots up to 1.5 Å resolution. Until now data sets of several biologically important materials have been collected by BIX-4, and their structural analyses are currently under way.

In conclusion, as mentioned above, BIX-4 shortens the collection time of diffraction data sets. In addition, since it is still difficult to get large crystals of proteins and other biological macromolecules, a higher performance of BIX-4 increases the possibility to apply neutron crystallography to such biomacromolecules.

We wish to thank Dr. T. Kohzuma (Ibaraki University, Japan) for supplement of sample crystals of cytochrome C' and discussion. This study is supported in part by 'Development of New Structural Biology Including Hydrogen and Hydration' in the Organized Research Combination System (ORCS) prompted by the Ministry of Education, Culture, Sports, Science and Technology of Japan.

References

Chatake, T., Kurihara, K., Tanaka, I., Adams, M. W. W., Jenney, F. E. Jr., Tsyba, I., Bau, R. & Niimura, N. (2002). *Supplement 1 to Appl. Phys.* **A74**, s1280-s1282.
Fujiwara, S., Karasawa, Y., Tanaka, I., Minezaki, Y., Yonezawa, Y. & Niimura, N. (1998). *Physica* **B241-243**, 207-209.
Haga, Y. K., Neriishi, K., Takahashi, K. & Niimura, N. (2002). *Nucl. Instru. Meth.* **A487**(3), 504-510.
Kurihara, K., Tanaka, I., Adams, M. W. W., Jenney, F. E. Jr., Moiseeva, N., Bau, R. & Niimura, N. (2001). *Supplement A to J. Phys. Soc. Jpn*. **70**, 400-402.
Niimura, N., Karasawa, Y., Tanaka, I., Miyahara, J., Akahashi, K., Saito, H., Koizumi, S. & Hidaka, M. (1994). *Nucl. Instru. Meth.* **A349**(2-3), 521-525.
Niimura, N., Tanaka, I., Karasawa, Y. & Minakawa, N. (1995). *Physica* **B213-214**(1-4), 929-931.
Niimura, N. (1999). *Curr. Opin. Struct. Biol*. **9**(5), 602-608.
Niimura, N., Chatake, T., Ostermann, A., Kurihara, K. & Tanaka, I. (2003). *Z. Kristallogr*. **218**(2), 96-107.
Ostermann, A., Tanaka, I., Engler, N., Niimura, N. & Parak F. G. (2002). *Biophy. Chem.* **95**(3),183-193.
Tanaka, I., Niimura, N. & Mikula, P. (1999*a*). *J. Appl. Cryst.* **32**(3), 525-529.
Tanaka, I., Kurihara, K., Haga, Y., Minezaki, Y., Fujiwara, S., Kumazawa, S. & Niimura, N. (1999*b*). *J. Phys. Chem. Solids* **60**(8-9), 1623-1626.
Tanaka, I., Kurihara, K., Chatake, T., Niimura, N. (2002). *J. Appl. Cryst.* **35**(1), 34-40.
Tsyba, I. & Bau, R. (2002). *Chemtracts*, **15**(5), 233-257.

 Received 30 April 2003 • Accepted 15 October 2003